Static forces weighted Jacobian motion models for improved Odometry

Javier Hidalgo-Carrio, Ajish Babu and Frank Kirchner[1]

Abstract— **The estimation of robot's motion at the *prediction* step of any localization framework is commonly performed using a motion model in conjunction with inertial measurements. In the context of field robotics, articulated mobile robots have complex chassis. They might require a complete model in comparison with the traditionally used planar assumption. In this paper, we use a Jacobian motion model-based approach for real-time inertial-added odometry. The work makes use of the transformation approach [1] to accurately model 6-DoF kinematics. The algorithm relates normal forces with the probability of a contact-point to slip. The result increases the accuracy by weighting the least-squares solution using static forces prediction. The method is applied to the Asguard v3 system, a simple but highly capable leg-wheel hybrid robot. The performance of the approach is demonstrated in extensive field testing within different unstructured environments. In-depth error analysis and comparison with planar odometry is discussed, resulting in a superior localization.**

I. INTRODUCTION

Localization focuses on determining the pose (i.e. position and orientation) with respect to a global coordinate frame and typically within a map. Probabilistic localization frameworks, as variants of Bayes filters, have been used to solve the localization problem [2], [3], [4]. Those frameworks fuse sensory data to propagate robot's pose while moving. The process is separated into *prediction* and *correction* of the pose using proprioceptive and exteroceptive sensors respectively.

The estimation of motion in the *prediction* step is commonly performed using a motion model. Motion models have real-time capabilities and are inexpensive in comparison with sophisticated map matching techniques. The inheritance from indoor robotics at the time robots were operating in structured "planar" environments brings simplistic techniques. However, this simplicity causes a performance degradation specially while localizing on complex uneven terrains. Therefore, extensive sensing capabilities have to overcome with a poor odometry performance.

In this paper we present a method that is able to *optimally*[2] combine the motion related to each contact point. Our approach is motivated by the observation that the robot has different normal forces at each contact point while moving. The primary contribution of our work is fusing, in a unified framework, normal forces with the probability of each contact to slip. A performance analysis also demonstrates that a complete motion model is more accurate than skid-steers models. Moreover, the influence of fusing normal forces is also investigated and compared with commonly used planar motion models. Related work is presented in the next section. The details of the proposed technique are described in Section III. Section IV contains the results for challenging large-scale unstructured environments. The method is applied to a particular rover, i.e. the Asguard platform [5] a capable but simple skid-steer leg-wheel platform. Conclusions and limitations of this work are mentioned at the end of the manuscript.

II. RELATED WORK

Odometry has been widely studied since many robots only rely in dead-reckoning processes for basic localization. Starting from a known pose, odometry involves the calculation of robot's body configuration from encoders readings. The disadvantage of dead-reckoning systems is very well-known. The localization uncertainty grows unbounded due to accumulation of errors. Considerable research has been done in order to reduce the undesirable effect of poor odometry performace. The literature focusses on three specific types of errors: (1) Systematic errors, such as misalignment of actuators and uncertainty about effective link dimensions (2) Non-systematic errors, which include slippage, dragging, forces and multi-point wheel contact models with the ground. (3) Numerical drift and linearization errors, due to discrete-time integration of delta-poses.

The elimination of systematic errors is described from early research [6]. Calibration methods were applied for specific trajectories in order to reduce the effect of unequal wheel diameter and uncertainty about the wheelbase (deterministic errors). A general method based on least-squares is proposed in [7] with no limitation to a particular predefined path. Differential-drive platforms are commonly discussed for indoor scenarios because they are mechanically simple to build. Position tracking in challenging terrains was also investigated in [8]. Simulations results are investigated for the Rocky7 rover in [9] defining the wheel contact angle and slip vector.

Slippage correction has been the main non-systematic error as it causes bad results affecting the final pose. Visual odometry techniques are used to overcome the effect of slippery terrains [10], [11]. Fuzzy logic has also been used to detect wheel slippage by comparing the motor current on the called FlexNav architecture [12]. Their work corrects wheel-slippage based on motor current measurements. They introduce a linearized function to relate electric current and

All authors are with the DFKI - Robotics Innovation Center, Robert-Hooke-Str. 1, 28359 Bremen, Germany
[1]Department of Mathematics and Informatics, University of Bremen, 28359 Bremen, Germany
{name}.{surname}@dfki.de

[2]Optimally here refers to the best estimated value from a weighted least-squares perspective.

wheel-terrain interaction [13]. Marcovitz *et al* [14] present a delayed state filter technique in combination with a vehicle system model to correct wheel slip. Adaptive odometry by means of terrain classification using inertial data has been investigated in [15]. A regression function is trained off-line to directly output the adaptive correction coefficient of the odometry model. A sensitivity analysis of the learned parameters was not discussed. Performance analysis for omnidirectional robots in rough terrain is available in [16]. Slip compensation based on wheel velocities differences is analyzed for a traditional skid-steer kinematics in circumference trajectories.

Nowadays, the localization problem requires a more elaborated analysis and understanding to identify the impact of motion models. As of today, the improvement evaluation of such impact is still an open issue. A field testing comparison of more sophisticated motion models for odometry motivates this manuscript.

III. STATISTICAL MOTION MODELS

Motion models together with attitude kinematics are the two main methods for odometry. Nowadays, many robotic applications combine both due to consistency over time. The attitude kinematics is self-sufficient with inertial sensors except for the less observable angle (i.e. the heading) [17]. Motion models are more accurate than double integration of accelerometers readings, specially when *tactical-grade* sensors are not affordable.

A. Kinematic Modeling

A minimum of two coordinate frames per kinematic chain are required: a robot body frame (B) attached to the desired rover center and a contact frame (C_{ij}) defined as a single point of contact between the robot and the ground. The rest of coordinate frames are the minimum required for the computation of the transformation matrix $T_{BC_{ij}}$ which relates frame (B) with frame (C_{ij}). It will depend on a particular kinematics and the number of joints represented by the vector $q = [q_0 \; q_1 \; ... \; q_n]$ where n is the number of degrees of freedom of the mechanism - see Fig. 1. The B frame is related to a fixed world frame (W) by the pose vector $U = u_{W,B} = (x \; y \; z \; \phi \; \theta \; \psi)$.

Outdoor robots navigate on uneven terrains. They require the definition of contact angles between the ground and the point in contact. Typically, one contact angle in the direction of motion is necessary for wheeled mobile robots δ_{ij} - see Fig. 2. Pure walking machines might require two angles at the point in contact (i.e. the gradients in the lateral and transversal direction). In addition, the motion of the contact point consists of a slip vector ε_{ij}, which is modeled in three dimensions. A translation in the x axis by ξ_{ij}, lateral slip η_{ij} along the y axis and rotational slip ζ_{ij} along the z axis ($\varepsilon_{ij} = [\xi_{ij} \; \eta_{ij} \; \zeta_{ij}]$).

Mobile robots are commonly commanded by desired velocities. The mapping between the rover Cartesian space rate vector $\dot{u} = \dot{u}_{\bar{B},B} = \begin{bmatrix}\dot{x} \; \dot{y} \; \dot{z} \; \dot{\phi} \; \dot{\theta} \; \dot{\psi}\end{bmatrix}$ and the joint space rate vector with the contact rate angle and slip rate vector is solved by the Jacobian matrix. Velocity kinematics is deduced by derivation of the transformation matrix. Defining the transformation of the rover body at time step $k-1$ ($\bar{B}$) to rover body at time step k (B) as $T_{\bar{B},B} = T_{\bar{B},\bar{C}_{ij}} T_{\bar{C}_{ij},C_{ij}} T_{C_{ij},B}$, the derivative is

$$\begin{aligned}\dot{T}_{\bar{B},B} = \dot{T}_{\bar{B},\bar{C}_{ij}} T_{\bar{C}_{ij},C_{ij}} T_{C_{ij},B} + \\ T_{\bar{B},\bar{C}_{ij}} \dot{T}_{\bar{C}_{ij},C_{ij}} T_{C_{ij},B} + \\ T_{\bar{B},\bar{C}_{ij}} T_{\bar{C}_{ij},C_{ij}} \dot{T}_{C_{ij},B}\end{aligned} \tag{1}$$

The resulting Jacobian matrix J_{ij} related to the contact point ij has the form

$$\begin{bmatrix}\dot{x} \; \dot{y} \; \dot{z} \; \dot{\phi} \; \dot{\theta} \; \dot{\psi}\end{bmatrix}^T = J_{ij} \begin{bmatrix}\dot{q} \; \dot{\varepsilon}_{ij} \; \dot{\delta}_{ij}\end{bmatrix}^T \tag{2}$$

It defines the contribution of each kinematic chain to the body motion allowing the analysis of each chain and contact point to the resulting final velocity in $\dot{u}$. Considering a single contact angle the J_{ij} matrix size is $6 \times (n+4)$ where n corresponds to the DoF of the mechanism. The composite rover equations are obtained combining the Jacobian matrices for all kinematics chains into a sparse matrix equation of appropriate dimensions.

$$\begin{bmatrix} I_{6\times6} \\ I_{6\times6} \\ \vdots \\ I_{6\times6} \end{bmatrix} \begin{bmatrix} \dot{x} \\ \dot{y} \\ \dot{z} \\ \dot{\phi} \\ \dot{\theta} \\ \dot{\psi} \end{bmatrix} = J \begin{bmatrix} \dot{q} \\ \dot{\varepsilon} \\ \dot{\delta} \end{bmatrix} \equiv S\dot{u} = J\dot{p} \tag{3}$$

Navigation kinematics relates the rover pose rates to joints and sensed rate quantities. The navigation kinematics is the input for statistical motion models and the basis for dead reckoning estimation. Robot's sensor availability defines sensed and non-sensed quantities and (3) separates into the following form:

$$\begin{bmatrix} S_s & S_n \end{bmatrix} \begin{bmatrix} \dot{u}_s \\ \dot{u}_n \end{bmatrix} = \begin{bmatrix} J_s & J_n \end{bmatrix} \begin{bmatrix} \dot{p}_s \\ \dot{p}_n \end{bmatrix} \tag{4}$$

Rearranging into non-sensed (left-side) and sensed (right-side) quantities, the resulting equation is obtained

$$\begin{bmatrix} S_n & -J_n \end{bmatrix} \begin{bmatrix} \dot{u}_n \\ \dot{p}_n \end{bmatrix} = \begin{bmatrix} -S_s & J_s \end{bmatrix} \begin{bmatrix} \dot{u}_s \\ \dot{p}_s \end{bmatrix} \equiv \Omega\nu = b \tag{5}$$

where Ω is the matrix whose dimensions depend on the sensing capabilities of the rover and directly influence the existence of a solution. The solution to the overdetermined system above is based on minimizing the error vector $E = e^T Ce$, where C encodes the individual contribution of each kinematics chain to the estimated solution

$$E = e^T Ce = (b - \Omega\nu)^T C (b - \Omega\nu) \tag{6}$$

The solution for the linearized problem in (6) provides a minimum error for the vector e. For further details on kinematic model development the reader is referred to [1], [9], [18].

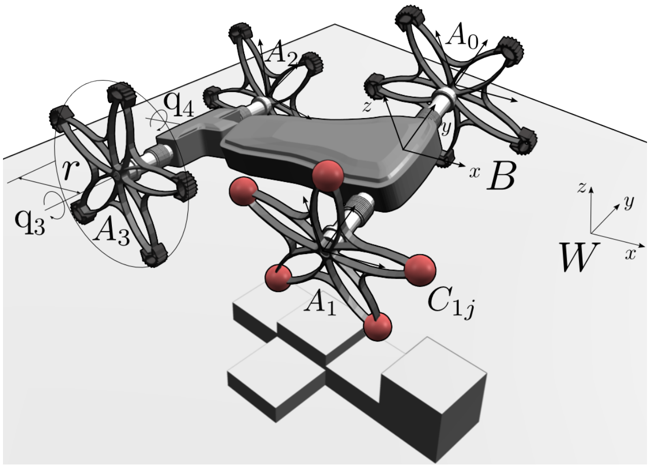

Fig. 1: Illustration of Asguard rover kinematics modeling. W is the world reference frame, B is the body frame located in the middle of the front axle, A_i is the wheel frame and C_{ij} the contact point frame. The pose estimation is computed as composite equation of wheel Jacobian matrices.

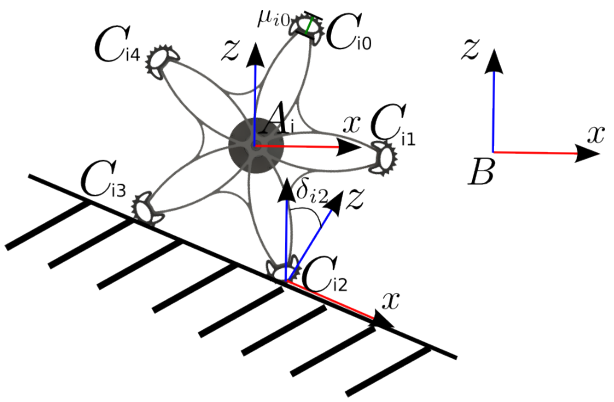

Fig. 2: Schematic representation of coordinate frames for the wheel i on an inclined terrain for hybrid leg-wheel systems. The contact angle is a key distinction between indoor and outdoor robots. While wheel's contact point is usually modeled in a constant position relative to the wheel axle for common rigid disc wheels, the assumption does not hold for a hybrid system.

B. Quasi-Static Forces Estimation

Computation of odometry is highly influenced by the amount of wheel slip, which in turn depends on the maximum usable tractive force between ground and the wheel. The maximum available traction [19], assuming a simple friction model, is proportional to the normal force on each wheel. The normal force distribution among the wheels of the robot is based on static reaction forces caused by the robot's weight. The computation of every sample time, based on the measured wheel positions and the estimated leg positions, hence called quasi-static force estimation.

It is assumed that the leg which is the lowest, in relation to the robot body plane, is in contact with the ground and coincident with the contact point frame C_{ij}. This assumption

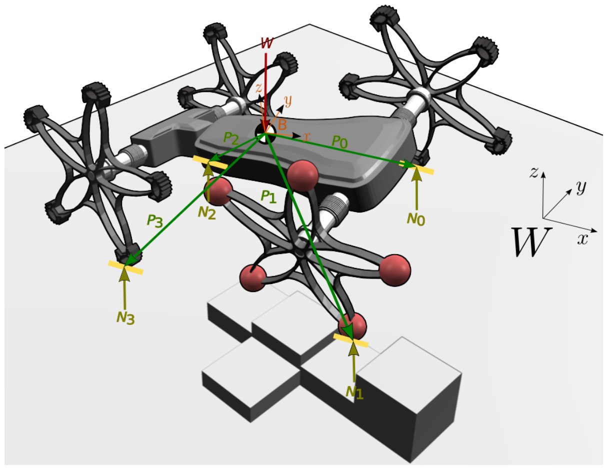

Fig. 3: Free body diagram for static force computations.

is mostly valid for relatively uneven surfaces. For highly uneven surfaces, it is possible that the higher feet is in contact with the ground and the lowest is not. In such scenarios, for a more accurate estimation, additional sensors need to be added to the feet to detect contact and forces [20]. Multiple feet can be in contact simultaneously as well but mainly a single foot is leading the motion.

The free body diagram for computation of static forces is given in Fig. 3. W is the world reference frame, B the body fixed reference frame with origin at the Center of Mass (CoM) and w is the weight of the robot acting along the gravity vector (z-axis of W). Let $i = \{0,1,2,3\}$, then N_i are the normal reaction forces from the ground due to the robot weight and P_i are the position vectors to the leg contact points. Henceforth the corresponding coordinate systems are added to the representations.

A new reference frame B' (not shown in the Figure) can be defined with the origin coinciding with the CoM of the robot, but aligned to W. The terms for $N_{B'i}$ and w in B' is given by,

$$N_{B'i} = \begin{bmatrix} 0 \\ 0 \\ n_i \end{bmatrix}, w = \begin{bmatrix} 0 \\ 0 \\ mg \end{bmatrix} \tag{7}$$

Where n_i are the scalar reaction forces along the z-axis of B', m is the mass of the robot and g is the acceleration due to gravity.

The objective is to derive the equations for the values of n_i. The equations are developed based on the fact that the robot has a free joint and this joint cannot transmit any torques. Therefore the torques in the front and the rear part of the robot along this free joint are independent. When the robot is quasi-static,

1) Sum of forces along the z-axis of B' equals the weight of the robot.

$$\Sigma n_i = mg \tag{8}$$

2) Sum of torques along the y-axis of B is zero.

$$\Sigma\left(P_{Bi} \times N_{Bi}\right)\big|_y = 0 \tag{9}$$

3) Sum of torques due to N_0 and N_1 along the x-axis of B is zero.

$$(P_{B0} \times N_{B0} + P_{B2} \times N_{B1})\,|_x = 0 \tag{10}$$

4) Sum of torques due to N_2 and N_3 along the x-axis of B is zero.

$$(P_{B2} \times N_{B2} + P_{B3} \times N_{B3})\,|_x = 0 \tag{11}$$

Let the rotation from B' to B and the position vector P_{Bi} be given by

$$R_{BB'} = \begin{bmatrix} r_{00} & r_{01} & r_{02} \\ r_{10} & r_{11} & r_{12} \\ r_{20} & r_{21} & r_{22} \end{bmatrix}, P_{Bi} = \begin{bmatrix} p_{ix} \\ p_{iy} \\ p_{iz} \end{bmatrix}, \tag{12}$$

Using (12), relationship between $N_{B'i}$ and N_{Bi} is given by,

$$N_{Bi} = R_{BB'} N_{B'i} = \begin{bmatrix} r_{02} \\ r_{12} \\ r_{22} \end{bmatrix} n_i \tag{13}$$

Computing torques from (12) and (13),

$$\tau_{Bi} = P_{Bi} \times N_{Bi} = \begin{bmatrix} p_{ix} \\ p_{iy} \\ p_{iz} \end{bmatrix} \times \begin{bmatrix} r_{02} \\ r_{12} \\ r_{22} \end{bmatrix} n_i \tag{14}$$

$$\tau_{Bi} = \begin{bmatrix} p_{iy} r_{iz} - p_{iz} r_{iy} \\ p_{iz} r_{ix} - p_{ix} r_{iz} \\ p_{ix} r_{iy} - p_{iy} r_{ix} \end{bmatrix} n_i \tag{15}$$

Using (15) let,

$$\begin{bmatrix} p_{iy} r_{iz} - p_{iz} r_{iy} \\ p_{iz} r_{ix} - p_{ix} r_{iz} \\ p_{ix} r_{iy} - p_{iy} r_{ix} \end{bmatrix} = \begin{bmatrix} t_{ix} \\ t_{iy} \\ t_{iz} \end{bmatrix} \tag{16}$$

Substituting (14), (15) and (16) in (9), (10) and (11), and combining them with (8) gives,

$$\begin{bmatrix} 1 & 1 & 1 & 1 \\ t_{0y} & t_{1y} & t_{2y} & t_{3y} \\ t_{0x} & t_{1x} & 0 & 0 \\ 0 & 0 & t_{2x} & t_{3x} \end{bmatrix} \begin{bmatrix} n_0 \\ n_1 \\ n_2 \\ n_3 \end{bmatrix} = \begin{bmatrix} mg \\ 0 \\ 0 \\ 0 \end{bmatrix} \tag{17}$$

The set of linear equations (17) can be solved for n_i by,

$$\begin{bmatrix} n_0 \\ n_1 \\ n_2 \\ n_3 \end{bmatrix} = \begin{bmatrix} 1 & 1 & 1 & 1 \\ t_{0y} & t_{1y} & t_{2y} & t_{3y} \\ t_{0x} & t_{1x} & 0 & 0 \\ 0 & 0 & t_{2x} & t_{3x} \end{bmatrix}^{-1} \begin{bmatrix} mg \\ 0 \\ 0 \\ 0 \end{bmatrix} \tag{18}$$

The reaction forces computed using (18) at every time step goes as input to the weighted Jacobian odometry model.

C. *Weighted Least-Squares of the Composite Equation*

A limitation of the kinematic model comes from the residual error E of the least-squares. Bad measurements might have a big penalty when minimizing the sum of the square of the errors. This case (e.g. a wheel is producing bad measurements because of poor traction) can be minimized by adjusting the matrix C in (6). How to *optimally* adapt the matrix while the robot interacts with the environment is performed by the quasi-static forces estimator described in the previous Section.

The matrix C is a sparse weighting matrix with block diagonal form. Each sub-matrix is a single wheel-weighting matrix for the contact point which is more likely to make contact with the ground. These sub-matrices are selected to have the structure $C_i = w_i I$ where w_i is the likelihood of each contact point to contribute to the resulting body motion. All wheels have equal probability to contribute to the motion for a perfect balance robot configuration (i.e.: $1/N$ per each contact point in contact with the ground C_{ij}, $\sum_i w_i = 1$). The quasi-static force estimator combines the attitude information coming from a Inertial Measurement Unit (IMU) to estimate the forces. Each estimated force is computed every delta-pose and the *instantaneous* probability per contact point is selected accordingly.

IV. EXPERIMENTAL RESULTS

The methodology was applied to the Asguard v3 system. Asguard is a simple yet highly capable hybrid system that is intended to serve as the scout rover unit in a multi-robot exploration scenario. It is able to navigate in complex uneven terrains and overcome demanding obstacles while maintaining a simple chassis mechanism (e.g.: skid-steer robots). It is instrumented with optimal encoders in each wheel and an absolute potentiometer for the passive joint. It is also equipped with GPS and a Sensonor STIM300 IMU including inclinometers, accelerometers and gyroscopes. When possible, GPS readings were corrected with a base station for more accurate positioning (e.g: RTK).

Inertial readings are sensed quantities in (5). The slip vector $\dot{\varepsilon}$ is not a sensed quantity and the contact point angles $\dot{\delta}$ are defined as unknown values even though some techniques could be used to estimate or measure these angles. Non-sensed quantities of the vector $\dot{u}$ are $\dot{x}$, $\dot{y}$ and $\dot{z}$. Here, the slip vector $\dot{\varepsilon}$ is modeled as only rotation along its z-axis ζ_i since it is assumed that the contact points slip with *non-holonomic* constraints.

Field testing with a rich variety of uneven terrains were selected to demonstrate the approach (see Fig. 4). The experiments consist of three different odometry calculations using on-board sensors readings from the encoders and the IMU. GPS, when available, was only used to post-process the correctness of the test. The proposed Jacobian odometry was computed with and without the weighting quasi-static forces and compared with a state of the art planar odometry. The planar odometry is a skid-steer odometry similar to the kinematic model described in [15].

(a) Pictures at the sand field

(b) DFKI's outdoors test track with the performed trajectory depicted as dotted line

(c) Panoramic view of the motocross track

Fig. 4: Some images of the scenarios used for the experiments

A. Quantitative Results

Table I and II present the Root Mean Square Error (RMSE) and final error trajectory for the sand field and motocross test. From these results the Jacobian Odometry appears to have significant performance. The X-Y error is improved when modeling completely the robot kinematics instead of implementing a planar assumption. The weighted Jacobian approach improves the RMSE in all directions. A Jacobian odometry is less accurate in the Z-direction than the planar odometry. However, it is significantly improved by weighted the composite equations using quasi-static forces. The fact that planar model only estimates translation velocities in the X-Y directions, influences the error in elevation. This is because in the planar case the error is only due to the drift in attitude.

Table III shows the final error at the DFKI's test track. GPS values were not available during this test. Poor satellite signal was sensed due to the narrow view of the test track between buildings. Nevertheless, the results still present improvements for the final pose (closed loop). The improvement is

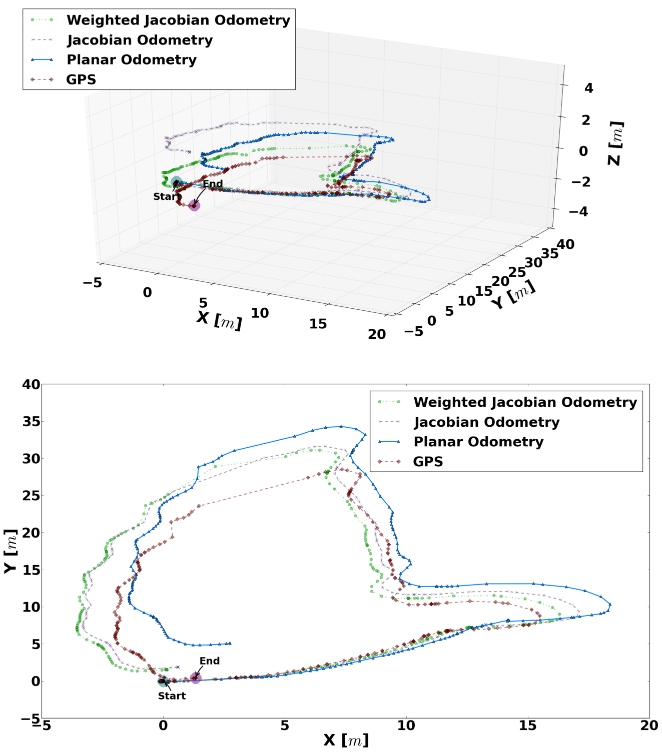

Fig. 5: Sand field test trajectory

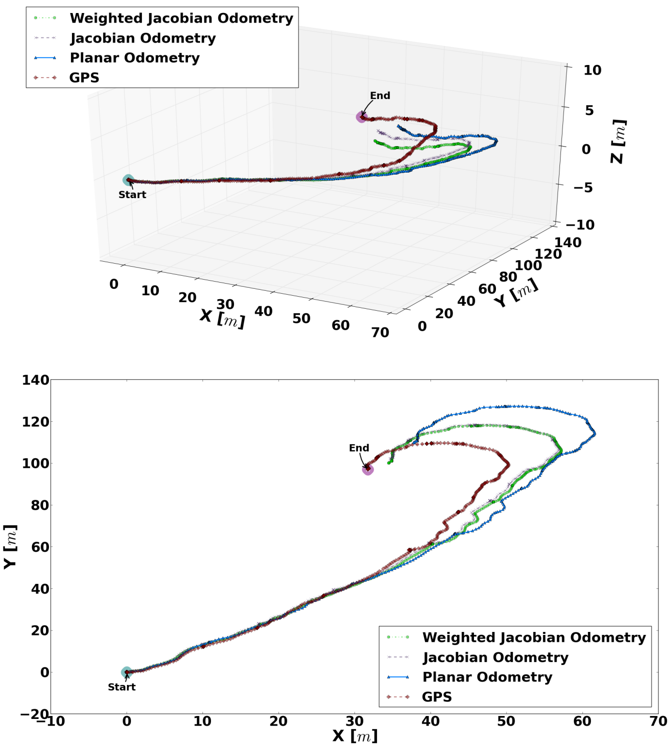

Fig. 6: Motocross test trajectory

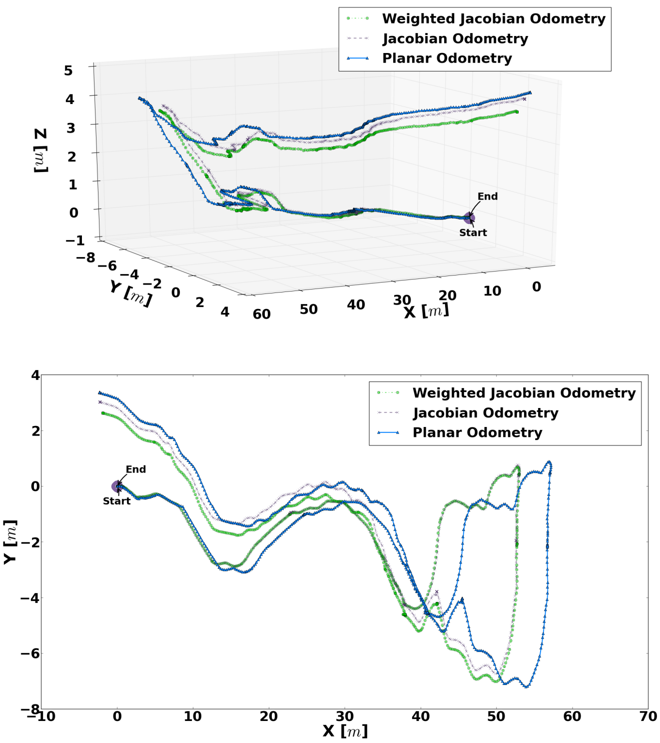

Fig. 7: DFKI's test track trajectory

TABLE I: Trajectory error for the Root Mean Square (RMS) and final error at the sand field

Method	RMSE $[m]$			Final $[m]$		
	x	y	z	x	y	z
Planar Odometry	0.94	3.39	0.93	1.43	4.65	1.95
Jacobian Odometry	0.89	1.59	2.14	0.73	1.47	3.18
Weighted Jacobian Odo.	0.84	1.08	0.39	1.18	1.10	0.78

TABLE II: Trajectory error for the Root Mean Square (RMS) and final error at the motocross track

Method	RMSE $[m]$			Final $[m]$		
	x	y	z	x	y	z
Planar Odometry	7.38	11.78	1.37	5.96	12.55	1.46
Jacobian Odometry	4.05	5.64	1.44	2.83	4.78	1.82
Weighted Jacobian Odo.	4.32	5.15	1.99	2.55	2.56	2.90

TABLE III: Trajectory error for the final error at DFKI's test track

Method	RMSE $[m]$			Final $[m]$		
	x	y	z	x	y	z
Planar Odometry	-	-	-	2.12	3.48	4.67
Jacobian Odometry	-	-	-	2.10	3.13	4.42
Weighted Jacobian Odo.	-	-	-	1.74	2.72	3.95

less significant than for the sand field and motocross areas since the terrain was mainly flat. Only when negotiating the bridge and climbing up the stairs a weighted Jacobian solution improves the localization performance.

Percentage error per distance travelled is compared for each different technique in Fig. 8. As a matter of importance, the bar chart shows the percentage error per each test as a function of the distance travelled. The planar odometry has 8.3% final error over a total distance of 168 m for the motocros test. The Jacobian and weighted Jacobian solution have 3.5% and 2.7% final error respectively for the same test. The sand field test comprises a total distance of 85 m. The proposed solution decreases from 6.1% down to 2.1% of the final error. The improvement is less significant at the DFKI's test tack, with 4.1% final error for a total distance travelled of 122 m. The error induced for the drift in pitch is dominant for this dataset. The RMSE comparison for the motocross and sand field tests are also shown in the bar chart of Fig. 9.

B. *Qualitative Results*

Fig. 5 and 6 depict qualitative results for the experiments when GPS was available. As expected, planar odometry suffer for lack of modeling while the Jacobian odometry estimates body motion more accurately. However, Jacobian odometry still has negative impact from wheels slippage and dragging. The weighted Jacobian solution better overcome with these negative effects. It is also appreciable in Fig. 7 that the pitch drift becomes dominant at DFKI's test track.

V. CONCLUSIONS

Motivated by the research during recent years and the interest of seeking better kinematics modelling, the work presented here improves the state of the art odometry models. We first compared acceptable planar odometry models versus full 6-DoF Jacobian models with representative field testing datasets. In addition to this, we proposed a modification of the technique by weighting the composite equation using quasi-static forces. The weighted Jacobian odometry while still simplistic in its modelling, shows an improvement in the localization error especially for challenging uneven terrains.

Force sensors at each contact point in order to accurately

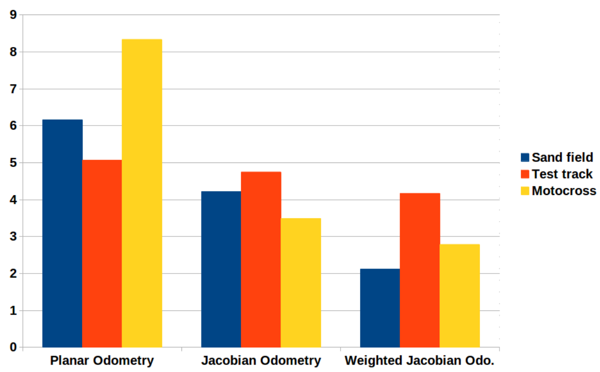

Fig. 8: Percentage error of the distance travelled per each test

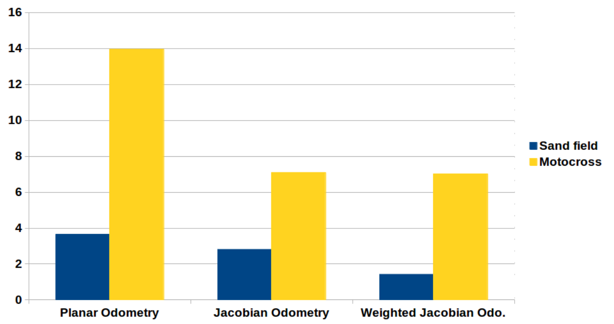

Fig. 9: Comparison of the Root Mean Square Error (RMSE) for the sand field and motocross (i.e: when GPS available) tests

estimate the interaction with the terrain is desirable for future improvements. Those extra sensors would help on accurately measuring normal forces as well as a better estimation of the contact angle δ_{ij}. Moreover, it will entail further leg-wheel developments.

REFERENCES

[1] P. F. Muir and C. P. Neuman, *Kinematic Modeling of Wheeled Mobile Robots*. Carnegie-Meloon University, 1986, no. June.

[2] S. Thrun, W. Burgard, and D. Fox, *Probabilistic Robotics*, ser. Intelligent robotics and autonomous agents series. Mit Press, 2005.

[3] M. Montemerlo, S. Thrun, D. Koller, and B. Wegbreit, "Faststlam: a factored solution to the simultaneous localization and mapping problem," in *Eighteenth national conference on Artificial intelligence*. Menlo Park, CA, USA: American Association for Artificial Intelligence, 2002, pp. 593–598.

[4] J. Schwendner, S. Joyeux, and F. Kirchner, "Using Embodied Data for Localization and Mapping," *Journal of Field Robotics*, pp. n/a–n/a, Nov. 2013.

[5] S. Joyeux, J. Schwendner, F. Kirchner, A. Babu, F. Grimminger, J. Machowinski, P. Paranhos, and C. Gaudig, "Intelligent Mobility - Autonomous Outdoor Robotics at the DFKI," *KI - Kuenstliche Intelligenz*, Feb. 2011.

[6] J. Borenstein and L. Feng, "Measurement and Correction of Systematic Odometry Errors in Mobile Robets," *IEEE Transactions on Robotics*, vol. 12, pp. 869–880, 1996.

[7] G. Antonelli, S. Chiaverini, and G. Fusco, "A Calibration Method for Odometry of Mobile Robots Based on the Least-Squares Technique : Theory," *IEEE Transactions on Robotics*, vol. 21, no. 5, pp. 994–1004, 2005.

[8] P. Lamon and R. Siegwart, "3D Position Tracking in Challenging Terrain," *The International Journal of Robotics Research*, vol. 26, no. 2, pp. 167–186, Feb. 2007.

[9] M. Tarokh and G. J. McDermott, "Kinematics Modeling and Analyses of Articulated Rovers," *IEEE Transactions on Robotics*, vol. 21, no. 4, pp. 539–553, 2005.

[10] D. Helmick, Y. Cheng, and S. Roumeliotis, "Path following using visual odometry for a Mars rover in high-slip environments," *IEEE Aerospace Conference Proceedings*, vol. 2, pp. 772–789, 2004.

[11] J. Rehder, K. Gupta, S. Nuske, and S. Singh, "Global pose estimation with limited GPS and long range visual odometry," *2012 IEEE International Conference on Robotics and Automation*, pp. 627–633, May 2012.

[12] L. Ojeda and J. Borenstein, "FLEXnav : Fuzzy Logic Expert Rule-based Position Estimation for Mobile Robots on Rugged Terrain BY," in *IEEE International Conference on Robotics and Automation*, no. May, 2002, pp. 1–6.

[13] L. Ojeda, D. Cruz, G. Reina, J. Borenstein, and S. Member, "Current-Based Slippage Detection and Odometry Correction for Mobile Robots and Planetary Rovers," *IEEE Transactions on Robotics*, vol. 22, no. 2, pp. 366–378, 2006.

[14] F. Rogers-marcovitz, M. George, N. Seegmiller, and A. Kelly, "Aiding Off-Road Inertial Navigation with High Performance Models of Wheel Slip," in *IEEE International Conference on Intelligent Robots and Systems*, 2012.

[15] M. Reinstein, V. Kubelka, and K. Zimmermann, "Terrain adaptive odometry for mobile skid-steer robots," in *2013 IEEE International Conference on Robotics and Automation*. IEEE, May 2013, pp. 4706–4711.

[16] G. Ishigami, E. Pineda, J. Overholt, G. Hudas, and K. Iagnemma, "Performance analysis and odometry improvement of an omnidirectional mobile robot for outdoor terrain," in *2011 IEEE/RSJ International Conference on Intelligent Robots and Systems*. IEEE, Sept. 2011, pp. 4091–4096.

[17] J. L. Crassidis and F. L. Markley, "Unscented filtering for spacecraft attitude estimation," *Journal of guidance, control, and dynamics*, vol. 26, no. 4, pp. 536–542, 2003.

[18] J. Hidalgo, "Navigation and Slip Kinematics for High Performance Motion Models," in *Symposium on Advanced Space Technologies in Robotics and Automation*, 2013.

[19] J. Y. Wong, *Theory of Ground Vehicles, 3rd Edition*. Wiley-Interscience, 2001.

[20] K. Fondahl, D. Kuehn, F. Beinersdorf, F. Bernhard, F. Grimminger, M. Schilling, T. Stark, and F. Kirchner, "An adaptive sensor foot for a bipedal and quadrupedal robot," in *2012 4th IEEE RAS & EMBS International Conference on Biomedical Robotics and Biomechatronics (BioRob)*. IEEE, June 2012, pp. 270–275.